

Study on the Stationkeeping Strategy for the Libration Point Mission

Toshinori Ikenaga¹⁾ and Masayoshi Utashima¹⁾

¹⁾Trajectory and Navigation Group, Japan Aerospace Exploration Agency, Japan

The Japan Aerospace Exploration Agency, JAXA, is now planning the next-generation infrared astronomical mission, called SPICA. SPICA is the first Japanese libration point mission to utilize a halo orbit around L2 in the Sun-Earth system. This paper describes the study on the stationkeeping strategy for such libration point mission. The main algorithm is structured with reference to the paper written by K. C. Howell et al. [1993]. In addition, to conduct a decade-long simulation, the long-term reference halo trajectory is produced by the method developed by M. Utashima [2005]¹⁾. Assuming the stationkeeping algorithm can be applied to SPICA, the attitude constraints of SPICA and frequent disturbances caused by the unloading operation of the reaction wheels are taken into consideration in this study.

ラグランジュ点ミッションにおける軌道保持手法に関する研究

池永敏憲¹⁾, 歌島昌由¹⁾

¹⁾宇宙航空研究開発機構 研究開発本部 軌道・航法グループ

JAXA は現在、次世代赤外線天文衛星 SPICA の概念設計を行っている。SPICA は太陽—地球系 L2 点周りのハロー軌道に投入される予定であるが、L2 点周りの軌道は不安定であるため、SPICA が予定しているミッション期間 5 年間に亘りハロー軌道にとどまるためには、軌道保持が必須となる。本論文では、K.C.Howell 氏の論文⁴⁾を基に軌道保持アルゴリズムを構築し、SPICA の太陽方向制約、 ΔV 制御誤差、ハロー軌道投入・決定誤差、RW アンローディング時に発生する並進 ΔV (アンローディング ΔV) を考慮した軌道保持を実施した。長期間の基準軌道の作成には、JAXA 歌島昌由氏が開発した、SQP 法を用いた長期間ハロー軌道の設計手法を利用した¹⁾。その解析結果を報告する。

1. Introduction

The Japan Aerospace Exploration Agency, JAXA, is now planning the next-generation infrared astronomical mission called SPICA. SPICA is the first Japanese libration point mission to utilize the halo orbit around Lagrange point 2 in the Sun-Earth system³⁾. Since the L2 libration point trajectories are unstable, some form of trajectory control is necessary to keep spacecraft (S/Cs) close enough to their nominal paths¹⁾.

This paper describes the study on the stationkeeping strategy assuming application to SPICA as an example of a libration point mission. The main stationkeeping algorithm is structured with reference to the paper written by K. C. Howell et al. [1993]⁴⁾, and to conduct the decade-long simulation, the long-term reference halo trajectory is produced by the method developed by M. Utashima [2005]¹⁾, which utilizes the Sequential Quadratic Programming, SQP method. In this study, the attitude constraint of SPICA and the frequent disturbances caused by the unloading operation of the reaction wheels (RWs)

are taken into consideration, and an optimal thruster allocation for a SPICA-like mission is proposed.

2. Force Model and Coordinate System

In this study, the Sun, Earth and Moon are taken into consideration and each orbit is precisely determined by DE405. The S/C's trajectory is also computed numerically, including the gravitational forces from those three celestial bodies. The coordinate system for the orbit propagation is the mean equator and equinox of J2000, and the coordinate system of a halo trajectory is the L2-centered rotational coordinate system⁸⁾.

3. Stationkeeping Algorithm

The main stationkeeping algorithm is constructed based on the paper written by K. C. Howell et al. [1993]⁴⁾. This algorithm is to minimize the sum of squares of the corrective delta-V and the deviation between the nominal and estimated trajectories at the two target epochs, t_1 and t_2 . Table 3-1 shows an explanation of each parameter.

Table 3-1. Parameters

t_{\min}	Minimum time interval of delta- V_c
Δt_1	Time interval between the planned delta- V_c execution time and the target time t_1
Δt_2	Time interval between the planned delta- V_c execution time and the target time t_2
t_{tracking}	Time interval to the execution of the next delta- V_c , if the planned delta- V_c is not executed
d_{\min}	Minimum position deviation
d_{\max}	Maximum position deviation
ΔV_{\min}	Minimum value of delta- V_c

Let us divide the state transition matrix (6 x 6) from the initial epoch t_0 to a certain time t ($t \geq t_0$) by 4 submatrices (3 x 3) as shown in Eq. (3-1).

$$\Phi(t, t_0) = \begin{bmatrix} A_{t_0} & B_{t_0} \\ C_{t_0} & D_{t_0} \end{bmatrix} \quad (3-1)$$

The deviation between the nominal and estimated trajectories at the epoch t_i ($t_i \geq t_0$) is defined as shown in Eq. (3-2).

$$\bar{m}_{t_i} \cong B_{t_i t_0} \bar{e}(t_0) + B_{t_i t_0} \Delta \bar{V}_c(t) + A_{t_i t_0} \bar{p}(t_0) \quad (3-2)$$

The three vectors $\bar{p}(t_0)$, $\bar{e}(t_0)$ and $\Delta \bar{V}_c(t)$ are the position deviation, velocity deviation at epoch t_0 and the corrective maneuver executed at epoch t ($t_i \geq t \geq t_0$), respectively. The corrective maneuver $\Delta \bar{V}_c(t)$ is computed by minimizing the cost function defined by Eq. (3-3).

$$J[\bar{p}, \bar{e}, \Delta \bar{V}_c] = \Delta \bar{V}_c(t)^T Q(t) \Delta \bar{V}_c(t) + \bar{m}_{t_1}^T R(t) \bar{m}_{t_1} + \bar{m}_{t_2}^T S(t) \bar{m}_{t_2} \quad (3-3)$$

The three matrices $Q(t)$, $R(t)$ and $S(t)$ are 3 x 3 weighting diagonal matrices.

The optimal corrective maneuver $\Delta \bar{V}_c(t)$ at epoch t is computed by setting the derivative of Eq. (3-3) by $\Delta \bar{V}_c$ equal to zero. The optimal corrective maneuver is described as shown in Eq. (3-4).

$$\Delta \bar{V}_c(t) = - \left(Q(t) + B_{t_1 t}^T R(t) B_{t_1 t} + B_{t_2 t}^T S(t) B_{t_2 t} \right)^{-1} \times \left[B_{t_1 t}^T R(t) B_{t_1 t_0} + B_{t_2 t}^T S(t) B_{t_2 t_0} \right] \bar{e}(t_0) + \left[B_{t_1 t}^T R(t) A_{t_1 t_0} + B_{t_2 t}^T S(t) A_{t_2 t_0} \right] \bar{p}(t_0) \quad (3-4)$$

4. Application to SPICA

4.1. Attitude Constraint

Since SPICA is an infrared astronomical mission with a cryogenically-cooled telescope, the attitude is severely constrained to keep the temperature extremely low. Fig. 4-1-1 shows the attitude constraint of SPICA around the x axis of the S/C body frame. There is no constraint around the y axis, while that around the z axis is $\pm 3^\circ$.

The thruster allocation of SPICA is undetermined, therefore two types of on-board thruster allocation are

taken into consideration in this paper. Fig. 4-1-2 shows both types of thruster allocations and the direction of the delta-V created in each thruster allocation.

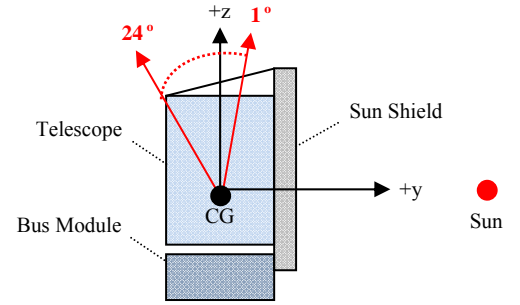


Fig. 4-1-1. Attitude Constraint of SPICA

In the “Type A” thruster allocation, the delta-V is created in the direction described as a red arrow in a) of Fig. 4-1-2 by simultaneous firing of the two thrusters on both sides. Conversely, the “Type B” thruster allocation has two trajectory control thrusters described as red triangles in b) of Fig. 4-1-2, which are attached to the lines connecting the barycenter of the S/C with the mounting point of the thrusters. This type of thruster allocation is employed by HERSCHEL of ESA⁷⁾. At this type of thruster allocation, the delta-V is created by firing the thruster of either side.

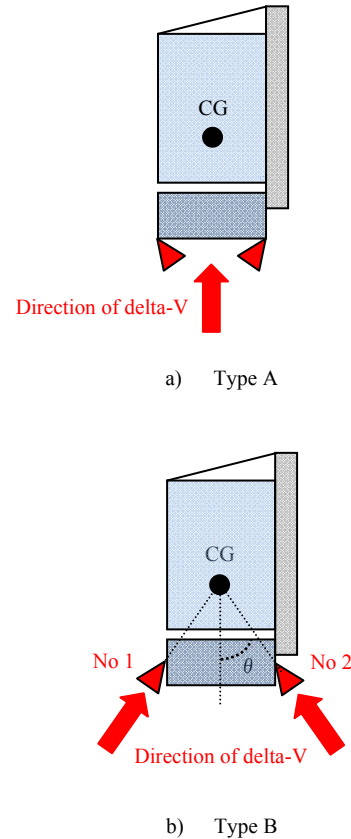


Fig. 4-1-2. Thruster Allocation

4.2. Unloading delta-V

In this study, the impact of the translational forces

(unloading delta-V) caused by the unloading operation of the on-board RWs is also investigated. The frequency of the unloading operation considered in this paper is daily, and the magnitude is 6.0 mm/s^6 .

The direction of the unloading delta-V is determined so as to eliminate the divergent component i.e. the eigenvector corresponding to the maximum eigenvalue of the state transition matrix of one period of the halo trajectory^{6), 8)}. This direction is called “stable delta-V direction”. The cant angle of the on-board thruster is considered to be 0 or 20° . Fig. 4-2-1 shows the definition of the cant angle of the thruster, and Fig. 4-2-2 describes the definition of the direction of the unloading delta-V.

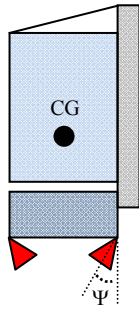


Fig. 4-2-1. Definition of the Cant Angle

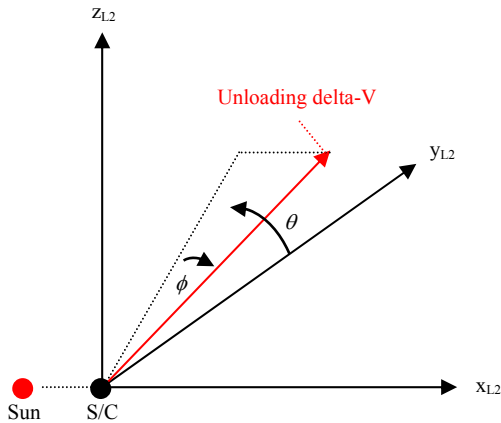


Fig. 4-2-2. Definition of the Unloading delta-V

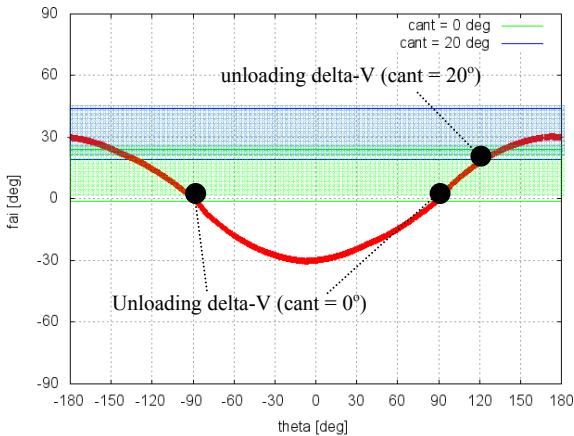


Fig. 4-2-3. Direction of the Unloading delta-V

In this study, the average stable delta-V direction is determined from the four different stable delta-V direction, which are computed from four different initial epoch and state vectors⁸⁾. Fig. 4-2-3 shows the relationship between the attitude constraint of each thruster cant angle and the stable delta-V direction, which is described as a red line in the figure. The green and blue areas of Fig. 4-2-3 denote the attitude constraint in the case of 0 and 20° cant angles, respectively.

In the case of the 20° cant angle, the direction in which the variance of the four “stable delta-V direction” is the smallest is chosen. Conversely, in the case of the 0° cant angle, two directions i.e. $\pm z_{L2}$ are chosen for the direction of the unloading delta-V. In this case, we assume the unloading delta-V direction changes alternately.

5. Reference Halo Trajectory

The long-term reference halo trajectory in this study is produced by the long-term halo trajectory design method developed by M. Utashima [2005]¹⁾.

5.1. Initial Halo Trajectory

Since the method used to produce the long-term reference halo trajectory uses the SQP method, an initial halo trajectory must be computed in advance. In this paper, the initial state values of each half revolution of the halo trajectory are computed based on the linear solution of the Circular Restricted Three Body Problem, CRTBP, and each half halo trajectory is connected to produce the initial halo trajectory. The half halo trajectories are defined as starting from the “xz” plane of the L2-centered rotational coordinate system and returning back to this plane. The connection points need not be continuous.

When we describe the initial state vector and the time of flight during the half revolution of the halo trajectory as $\mathbf{X}_0 = (x_0, y_0, z_0, u_0, v_0, w_0)^T$ and T , respectively, the algorithm to produce the initial halo trajectory is described as follows:

Algorithm for the Initial Halo Trajectory

1) Initial Condition

- $y_0 = 0$
- $z_0 = \text{designated}$
- $u_0 = 0$
- $w_0 = 0$

2) Unknown Parameters

- x_0, v_0, T

3) Termination Condition

- $y_T = 0$
- $u_T = 0$
- $w_T = 0$

The initial three unknown parameters are given from the linear solution of CRTBP and solved by the Newton Raphson method. The initial parameters are obtained from the following:

$$x_0 = \frac{A_y}{4.5}, z_0 = A_z, \dot{y}_0 = (1.7e - 6)x_0 \quad (5-1-1)$$

A_z is the designated value, which is $3.0e+5$ km in this paper. $A_y(e+5$ km) and $A_z(e+5$ km) have the following relationship:

$$A_y = \sqrt{1.364 A_z^2 + 4573} \quad (5-1-2)$$

5.2. Reference Halo Trajectory

The initial halo trajectory produced previously has position and velocity gaps at the connecting points of the half halo trajectories. These gaps are in the order of $1.0e+5$ km in position and 10 m/s in velocity, respectively. Since these gaps are not acceptable for the stationkeeping simulation, the SQP method is used to reduce the gaps. The control parameters, equality constraint and objective function are as follows:

SQP method

1) Control Parameters

$$\cdot x_0^i, z_0^i, u_0^i, v_0^i, w_0^i, \Delta t^i \quad (i = 1 \sim \text{NHREV})$$

2) Equality Constraint

$$\begin{aligned} \cdot x_f^i &= x^{i+1} & (i = 1 \sim \text{NHREV}-1) \\ \cdot y_f^i &= 0 & (i = 1 \sim \text{NHREV}) \\ \cdot z_f^i &= z^{i+1} & (i = 1 \sim \text{NHREV}-1) \\ \cdot u_f^i &= u^{i+1} & (i = 1 \sim \text{NHREV}-1) \\ \cdot v_f^i &= v^{i+1} & (i = 1 \sim \text{NHREV}-1) \\ \cdot w_f^i &= w^{i+1} & (i = 1 \sim \text{NHREV}-1) \end{aligned}$$

3) Objective Function

$$\frac{1}{2} \sum_{k=1}^{\text{NHREV}-1} (z^{2k+1}_0 - z^1_0)^2 \Rightarrow \min \quad (5-2-1)$$

“NHREV” is the number of half revolutions of the halo trajectory, and the initial, terminal state vectors and the time of flight of the i^{th} half halo trajectory are $\mathbf{X}_0^i = (x_0^i, y_0^i, z_0^i, u_0^i, v_0^i, w_0^i)^T$, $\mathbf{X}_f^i = (x_f^i, y_f^i, z_f^i, u_f^i, v_f^i, w_f^i)^T$ and Δt^i , respectively.

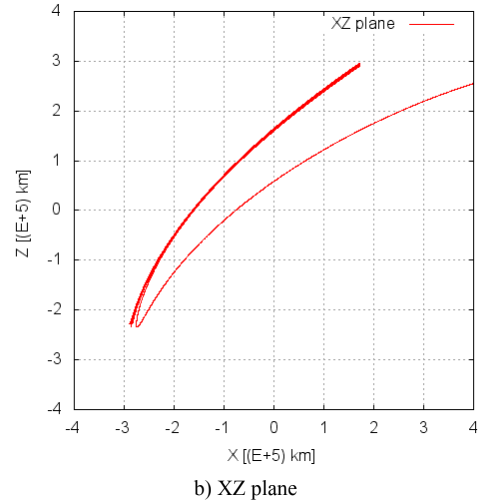
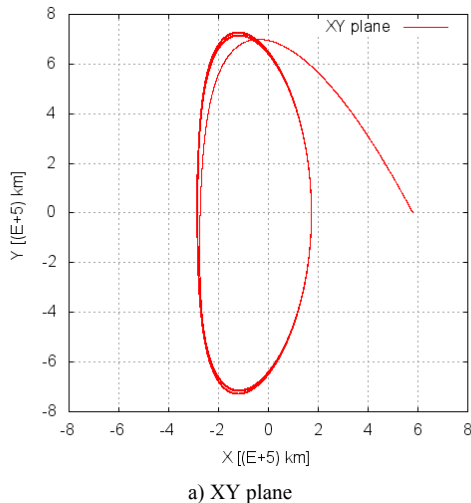


Fig. 5-2-1. Reference Halo Trajectory

Fig. 5-2-1 shows the reference halo trajectory. The duration of the reference trajectory is 3780 days while that of the stationkeeping simulation is 3600 days. The last half halo trajectory (after 3690 days) deviates largely from the halo trajectory, however the duration of the reference halo trajectory produced here has sufficient margin, meaning no problem for the stationkeeping simulation.

6. Stationkeeping Analysis

6.1. Configuration

In this study, we deal with three trajectories i.e. the “nominal” trajectory, which is the reference halo trajectory, the “actual” trajectory, in which the S/C flies, and the “estimated” trajectory, which the ground S/C operator can know by the orbit determination (O/D). Fig. 6-1-1 shows the relationship between these three trajectories.

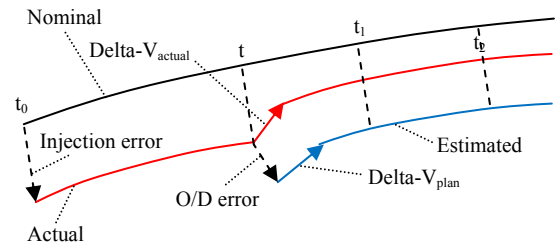


Fig. 6-1-1. Relationship between “nominal”, “actual” and “estimated” trajectories

As shown in Fig. 6-1-1, the injection error is applied at epoch t_0 to the “nominal” trajectory to produce the “actual” trajectory. Additionally, the O/D error is applied to the “actual” trajectory, which produces the “estimated” trajectory. Table 6-1-1 summarizes the detail of the injection and O/D errors.

In addition to the injection and O/D errors, the delta-V control error is also considered in this study. The attitude error is $0.167^\circ(1\sigma)$, and the magnitude error is $2.5\%(1\sigma)$.

Table 6-1-1. Injection and O/D error (L2-centered rotational coordinate system)

	X	Y	Z
Position (km)	1.5	2.5	15.0
Velocity(mm/s)	1.0	1.0	3.0

Table 6-1-2 summarizes the configuration of the stationkeeping analysis conducted in this paper.

Table 6-1-2. Configuration

Duration	360 days
t_{min}	30 days
Δt_1	4 days
Δt_2	65 days
$t_{tracking}$	2 days
d_{min}	0 km
d_{max}	5.0e+4 km
Q	Diag (5.0e+12, 3.0e+13, 1.0e+13)
R	Diag (1.0, 0.0, 1.0)
S	Diag (1.0, 1.0, 1.0)
ΔV_{min}	0.01 m/s

6.2. Analysis

In this study, we conduct a hundred simulations in each case, changing the “seed” to the random number generator and calculate the average and standard deviation.

Analysis 1: Evaluation of the feasibility of the algorithm

Initially, the feasibility of the stationkeeping algorithm is evaluated. In this analysis, the attitude constraint and the unloading delta-V are not considered however the injection error, O/D error and delta-V control error are taken into consideration.

Table 6-2-1 shows the total amount of the corrective delta-V of 3600 days (almost decade-long) simulation. The μ is the average and the σ is the standard deviation.

Table 6-2-1. Result of Analysis 1

μ m/s	σ m/s	$\mu+2\sigma$ m/s
0.776	0.055	0.831

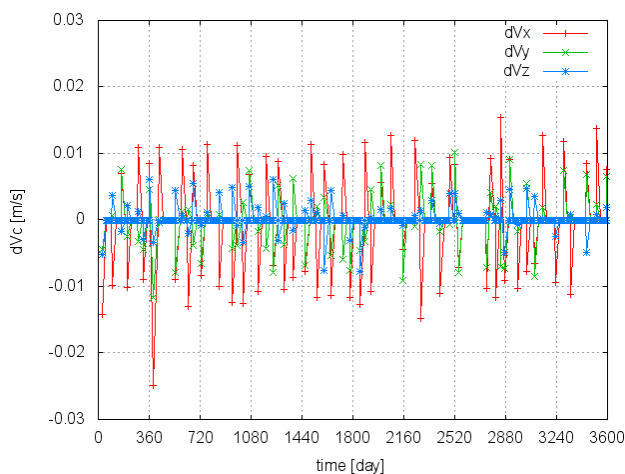


Fig. 6-2-1. Direction of Corrective Maneuver (L2-centered rotational coordinate system)

As shown in Table 6-2-1, the total amount of corrective delta-V of decade is very small i.e. 0.831 m/s in $\mu+2\sigma$.

Based on this result, we can deem the stationkeeping algorithm employed in this study sufficiently feasible.

Fig. 6-2-1 shows the direction of the corrective delta-V in the L2-centered rotational coordinate system. As the figure shows, $\pm x_{L2}$ directions dominate as the direction of the corrective delta-V, which means the direction of the corrective delta-V is almost on a line from the Sun to the L2 point.

Analysis 2: Influence of Attitude Constraint

In this analysis, the influence of the attitude constraint of SPICA is evaluated. As mentioned in the previous chapter, two types of on-board thruster allocation are taken into consideration. The injection error, O/D error and delta-V control error are taken into consideration, however the unloading delta-V is not considered in this analysis. Table 6-2-2 shows the results of this analysis.

Table 6-2-2. Results of Analysis 2

a) Type A		
μ m/s	σ m/s	$\mu+2\sigma$ m/s
30.499	9.215	48.929

b) Type B		
μ m/s	σ m/s	$\mu+2\sigma$ m/s
0.944	0.075	1.094

As is clear, the total amount of corrective delta-V of the “Type A” is huge. When we compare the total of the corrective delta-V of a decade with the value of $\mu+2\sigma$, it is about 45 times larger than that of the result of “Analysis 1”. Conversely, the total amount of “Type B” is small and almost the same as the result of the “Analysis 1” i.e. only 1.3 times larger.

Analysis 3: Influence of Unloading delta-V

This analysis includes all the factors which should be considered to simulate the “real” situation. In addition to the “Type A” and “Type B” thruster allocation, two cases of the thruster cant angle are taken into consideration to compare the influence of the unloading delta-V. First, Table 6-2-3 shows the result of this analysis in the case of a 20° cant angle. In this case, the direction of the unloading delta-V is constant.

Table 6-2-3. Results of Analysis 3 (20° cant angle)

a) Attitude constraint is <u>not</u> considered		
μ m/s	σ m/s	$\mu+2\sigma$ m/s
11.422	0.419	12.260

b) Attitude constraint is considered (Type A)		
μ m/s	σ m/s	$\mu+2\sigma$ m/s
779.500	565.786	1911.072

c) Attitude constraint is considered (Type B)		
μ m/s	σ m/s	$\mu+2\sigma$ m/s
14.339	0.626	15.591

As shown in Table 6-2-3, the total of the corrective delta-V of “Type A” is extremely large i.e. 1911 m/s,

which is obviously unacceptable because the maximum total delta-V of SPICA is about 113 m/s⁸⁾. Conversely, the total of “Type B” is about 16 m/s, which is small enough.

Secondly, Table 6-2-4 shows the result of this analysis in the case of a 0° cant angle. As mentioned in section 4-2, in the case of a 0° cant angle, the direction of the unloading delta-V changes in $\pm z$ directions in the L2-centered rotational coordinate system alternately.

Table 6-2-4. Results of Analysis 3 (0° cant angle)

a) Attitude constraint is not considered

μ m/s	σ m/s	$\mu+2\sigma$ m/s
0.785	0.075	0.935

b) Attitude constraint is considered (Type A)

μ m/s	σ m/s	$\mu+2\sigma$ m/s
30.811	12.159	55.129

c) Attitude constraint is considered (Type B)

μ m/s	σ m/s	$\mu+2\sigma$ m/s
0.947	0.065	1.077

Similar to the results of the previous analysis, the total of the corrective delta-V of “Type A” peaks among all three cases. However, in the case of a 0° cant angle, the total of “Type A” is about 55 m/s, which, although large, is still acceptable. Conversely, the total of “Type B” is only 1.0 m/s, which is negligible and only 1.3 times larger than that of case a), in which the attitude constraint is not considered.

7. Conclusion

In this study, the stationkeeping algorithm is structured with reference to the paper written by K. C. Howell et al.⁴⁾ and the feasibility of the algorithm is evaluated through certain cases of the stationkeeping simulation assuming the application of the algorithm to SPICA. In addition, to conduct a decade-long stationkeeping simulation, the long-term reference halo trajectory is produced by the long-term halo trajectory design method developed by M. Utashima¹⁾. From the results of the analyses, the following is revealed:

- 1) The $\pm x$ directions in the L2-centered rotational coordinate system dominate as the direction of the corrective delta-Vs.
- 2) The influence of the attitude constraint of SPICA can be reduced by choosing the proper on-board thruster allocation. In fact, from the results of the “Analysis 2” in the section 6-2, the total of the corrective delta-V of “Type A” is about 49 m/s, while that of “Type B” is about 1 m/s.
- 3) The frequent unloading delta-Vs increase the total corrective delta-V dramatically in the case of “Type A” and a 20° cant angle. The total of this case is about 1911 m/s, which is excessive for SPICA in terms of the on-board propellant. Conversely, in the case of the “Type B” and 0° cant angle, the total corrective delta-V is only 1 m/s.

As future works, the effect of the “Global Suppression Approach” developed and proposed by M. Nakamiya⁷⁾ to suppress the influence of the frequent unloading delta-Vs will be evaluated. Additionally, the influence of the solar radiation pressure will also be evaluated.

References

- 1) Masayoshi Utashima: *Design of Reference Halo Trajectories around L2 Point in the Sun-Earth System (Japanese)*, JAXA Research and Development Report, JAXA-RR-05-008, 2005
- 2) Masayoshi Utashima: *Orbital Mechanics Near Lagrange’s Points (Japanese)*, National Space Development Agency of Japan (NASDA) Technical Memorandum, NASDA-TMR-960033, 1997
- 3) SPICA Working Group: *SPICA Mission Proposal ver2 (Japanese)*, ISAS, JAXA, 2007
- 4) K. C. Howell, and H. J. Pernicka: *Stationkeeping Method for Libration Point Trajectories*, JOURNAL OF GUIDANCE, CONTROL and DYNAMICS, January-February (1993), vol.16, No1.
- 5) Oliver Montenbruck, Eberhard Gill: *Satellite Orbits, Models Method and Applications*, Springer, 2005
- 6) Masaki Nakamiya, Yasuhiro Kawakatsu: *Preliminary Study on Orbit Maintenance of Halo Orbits under Continuous Disturbance*, 20th AAS/AIAA Space Flight Mechanics Meeting 2010, AAS-10-119
- 7) Rainer Bauske: *Operational Maneuver Optimization for The ESA Mission HERSCHEL and PLANK*, 21st ISSFD, Toulouse, 2009
- 8) Toshinori Ikenaga, Masayoshi Utashima: *Study on the Stationkeeping Strategy for the Libration Point Mission*, 28th ISTS, 2011